RESEARCH ARTICLE

European Journal of Soil Science WILEY

Rhizosphere development under alternate wetting and drying in puddled paddy rice

Md. Dhin Islam[1,2] | Adam H. Price[1] | Paul D. Hallett[1]

[1]School of Biological Sciences, University of Aberdeen, Aberdeen, UK

[2]Faculty of Agriculture, Bangabandhu Sheikh Mujibur Rahman Agricultural University, Gazipur, Bangladesh

Correspondence
Md. Dhin Islam, Faculty of Agriculture, Bangabandhu Sheikh Mujibur Rahman Agricultural University, Room 107, Post Graduate Building, Gazipur-1706, Bangladesh.
Email: dhinislam@bsmrau.edu.bd

Abstract

Alternate wetting and drying (AWD) irrigation can save large amounts of water in rice cultivation. By repeatedly wetting and drying the soil under AWD, accentuated pore structure of the rhizosphere compared to flooded rice may occur. This could affect root growth and resource capture, but to date the physical structure and behaviour of the rhizosphere of rice under AWD has not been explored. In a controlled glasshouse experiment, two different textured soils were used in split rhizotrunks to separate a root-zone from bulk soil using mesh. To mimic a paddy field, the top of the rhizotrunk was filled with puddled soil and below the puddled layer there was a sieved soil layer. Root-zone physical properties were measured using a combination of high resolution X-ray CT imaging (pore structure), a miniaturised infiltrometer (hydrological) and a small indenter (mechanical). Soil under AWD irrigation had 46% greater macroporosity and 20% more pore connectivity compared to continuous flooding (CF). Compared to the bulk soil, root-zone soil under AWD or CF had greater macroporosity, water sorptivity and mechanical hardness. In the root-zone, AWD compared to CF increased the rate of water absorption by around 36%, but did not affect mechanical hardness. Our results suggest AWD interacting with rice roots could promote more effective water transmission through a more stable, larger and better-connected pore system. The results of this study also suggest that soil physical changes by AWD could improve the utilization of resources in a rice production system.

KEYWORDS
alternate wetting and drying, hydromechanics, macropore, rice, root-zone, soil structure

1 | INTRODUCTION

More than 75% of rice is produced under irrigated lowland continuous flooded (CF) puddled conditions (Lampayan et al., 2015), requiring 2–4 times more water per yielded rice than upland rice production (Bouman, 2009). Different water saving technologies in rice production are being explored to increase the water use efficiency and decrease greenhouse gas emissions. By far the most popular and promising is alternate wetting and drying (AWD) (Belder et al., 2004; Chidthaisong et al., 2018). In this system, rather than CF aided by

irrigation water, the soil is allowed to dry out gradually until the water table drops a shallow distance below the soil surface (Belder et al., 2004). After this drying, the soil is flooded again and the cycles repeated.

AWD can save 24%–38% of water over flooded production, but retain (Yao et al., 2012) or even increase (12%–15%) yields (Norton et al., 2017). A few studies have found a yield penalty, due to reduced vegetative growth of shoots and roots, but the amounts are small (1.8%–8.7%) compared to water savings (Bouman & Tuong, 2001; Carrijo et al., 2016). The drying stress from AWD can increase bulk density by the consolidation of soil (Fang et al., 2018), which can interact with the drier soil moisture to increase penetration resistance in the field (Norton et al., 2017). On rewetting dried paddy soil under AWD, soil strength increases may be irreversible (Yoshida & Hallett, 2008).

With cycles of wetting and drying of the soil under AWD, soil structure develops in an initially puddled and flooded soil due to shrinkage and cracking of the soil (Fang et al., 2018). At smaller scale, at the interface between the root and soil in the rhizosphere, drying stresses will be exacerbated compared to bulk soil due to plant water uptake. These drying stresses coupled with rhizodeposition and microbial processes are known to drive rhizosphere formation. Under mild AWD, typical to practices in most fields, organic acid production by rice roots can increase by up to 80% (Liang et al., 2020), providing exudates that influence rhizosphere structure development (Hallett et al., 2022). No studies have explored how AWD affects rhizosphere soil physical properties in rice. If AWD promotes improved transport properties and mechanical stability in the rhizosphere of rice, this could enhance resource capture and help explain yield benefits that have been observed.

The soil physical properties of the rhizosphere are most important among all other soil properties because they determine water and nutrients uptake (Aravena et al., 2011) by the plant roots and also can increase microbial activity (Cui & Holden, 2015) by improving aeration (Niu et al., 2012). This counters the effect of compaction of soil by the growing root, particularly if the soil wets and dries (Koebernick et al., 2017). From imaging of soil structure with X-ray CT, Aravena et al. (2011) found that the porosity of the rhizosphere reduced by 8%–12% compared to bulk soil for sweet pea and sunflower, having a negative impact on the hydraulic properties. Similarly, around 23% less porosity was recorded by Bruand et al. (1996) for a maize rhizosphere soil compared to bulk soil. On the other hand, Helliwell et al. (2017) found that the porosity increased by 18% in sandy loam and 30% in clay loam rhizosphere soil at a resolution compared to soil away from tomato roots. Several other studies have visualised rhizosphere soil structure

Highlights
- Soil physical structure and properties of the rhizosphere of rice under alternate wetting and drying (AWD) need to be explored.
- Due to wetting and drying the soil under AWD can change pore structure of the rhizosphere compared to continuous flooded rice.
- Soil of root-zone has greater macroporosity, water sorptivity and mechanical hardness compared to bulk soil.
- Soil physical changes by AWD can enhance resources utilization in rice production system.

(Koebernick et al., 2017; Mooney et al., 2012; Pires et al., 2019) and some have extended this to image based modelling to demonstrate improved physical conditions for plant growth (Cooper et al., 2018). In addition to compacting soil, root growth can also generate macropores as biopores from decomposed roots (Islam et al., 2023) and elongated cracks from axial expansion (Bodner et al., 2014). These elongated pores can affect bulk pore structure in soils, providing pathways for eased root growth of rice roots into the subsoil (Islam et al., 2021). From this research, it would be expected that AWD could enhance pore structure development in the rhizosphere, with benefits to plants.

Assuming AWD alters the soil pore structure in the rhizosphere, the soil hydrological properties may also change but results from studies on other species are contradictory. In wheat, the rhizosphere has been observed to be wetter compared to bulk soil (Young, 1995). Other research has found rhizosphere soil to be more water repellent than bulk soil, thereby decreasing the water absorption rate, but these effects are species dependent (Hallett et al., 2003). Further research with neutron radiography revealed that the water content in the rhizosphere was not constantly wetter or drier compared to bulk soil, but it depends on wetting and drying status of the soil (Carminati et al., 2010). With AWD applied to rice, the research reviewed thus far suggests that in the rhizosphere, increased water transport from pore structure development could be mediated by water repellency resulting from rhizodeposition.

Along with soil structural and hydrological properties, the plant root can increase soil mechanical stability of the rhizosphere (Moreno-Espíndola et al., 2007). This arises from particle bonding by root exudates and mucilage and localised compaction (Aravena et al., 2011; Dexter, 1987). Rhizosphere compaction can be beneficial for the plant roots by improving hydraulic contact among soil aggregates and by preserving soil connectivity, thereby improving

aeration and infiltration (Berli et al., 2008; Carminati et al., 2008). However, with wetting and drying stresses, rhizosphere structure can de-compact through aggregation of the soil particles (Koebernick et al., 2017). Under AWD, this mechanical loosening would be expected.

Strong evidence therefore exists to suggest that AWD, compared to the conventional approach of CF, could improve the physical properties of the rhizosphere of rice. Microscale tests are available to obtain direct hydrological and mechanical tests at the root–soil interface (Naveed et al., 2018). These approaches have demonstrated barley root hairs to increase water transport and decrease mechanical hardness. With these approaches, combined with X-ray CT, we test the hypothesis that AWD enhances the physical properties of the rice rhizosphere at the microscale. This has implications to resource capture and plant stress, possibly providing one explanation for improved plant performance that is sometimes observed under AWD. Rice was grown in split-rhizotrons consisting of rooted and non-rooted compartments, separated by a mesh. After 4 weeks growth under either simulated AWD or CF conditions, the split-rhizotrons were separated to expose the root system. This study focused on microscale hydrological and mechanical tests, coupled with high resolution X-ray CT imaging for structural development in the rhizosphere to test the following hypotheses: (i) macroporosity, pore size and pore connectivity will be greater in the root-zone because of the formation of cracks and aggregation due to root growth; (ii) AWD will improve soil macroporosity, connectivity due to shrinking and swelling of the soil; (iii) water sorptivity will decrease in the root-zone due to water repellency driven by the release hydrophobic exudates by the rice roots and microbial decomposition of these compounds; (iv) the soil hardness and elasticity will be greater in root-zone due to exudates from rice roots bonding and aggregating the soil and (v) the impacts of all rhizosphere changes will be greater in coarser textured soil because of the lower surface area and less bonding by clays.

2 | MATERIALS AND METHODS

2.1 | Soil and plant materials

The soil used in this experiment was collected from two fields of different soil textures. Sandy loam (71% sand, 21% silt and 8% clay) soil was sampled from a commercial farm in Insch, Aberdeenshire, UK. This soil is a Dystric Cambisol, with 0.34% N and 3.82% C. An alluvial silty clay loam soil (18% sand, 44% silt and 38% clay) was collected from a commercial farm in Inchture, Scotland, UK. The soil is a Eutric Stagnosol, with 0.28% N and 3.18% C. At both locations the sampling depth was 0–20 cm. Then soils from both locations were air dried to 0.15 g g^{-1}

moisture content to facilitate sieving using a roller sieve (2 mm). Soil nitrogen and carbon content were measured with a CNS elemental analyser (CE Instruments, Wigan, UK). The texture of the soils was determined by the hydrometer method (Gee & Bauder, 1986). The Insch soil was used in previous study for understanding the root–soil interaction for rice (Shrestha et al., 2014). The deep rooting Black Gora (an aus type from the Rice Diversity Panel 1 [Zhao et al., 2011]) rice genotype was used in this study.

2.2 | Experimental design and growth conditions

To enable exposure of the root–soil interface with minimal damage to the soil, the rice was grown in split rhizotrunks. This provided one side that contained the plant and roots, separated with 40 μm mesh from another side to constrain the roots but not the root exudates and mucilage. Figure 1 shows the rhizotrunk design. It was 4.3 cm wide, 5 cm deep and 30 cm high (volume was 645 cm^3). Soil was put into the rhizotrunk from the top, with the mesh barrier already secured. This was to compact the soil against the mesh during packing so that there
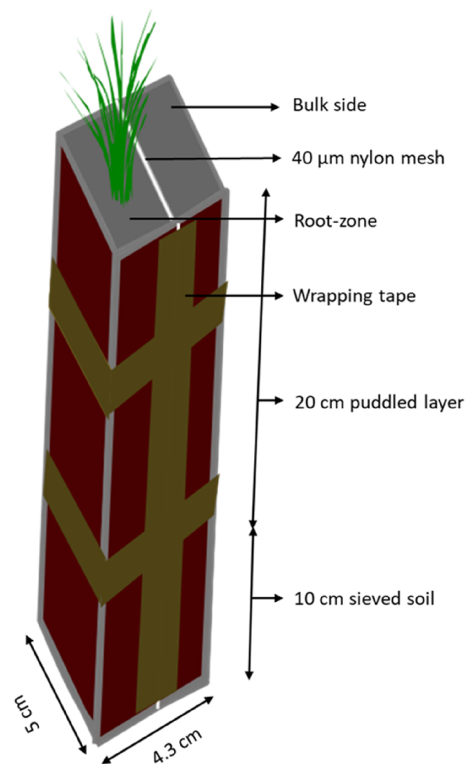
FIGURE 1 Schematic diagram of the split-rhizotrunk set-up. The rooted and bulk soil sides of the rhizotrunk were separated by placing a sheet of 40 μm nylon mesh vertically. The rhizotrunk halves were sealed together securely using a wrapping tape and rice seedling was planted in one half.

was contact between both sides of the rhizotrunk. The bottom 10 cm was packed with sieved soil at 20% moisture and a bulk density of 1.12 g cm^{-3}. Above the bottom, the top 20 cm was filled with puddled soil. Puddling involved mixing soil with water at 0.75 g g^{-1} moisture content and mechanically disrupted using a Kenwood mixer for 4 minutes with an agitator shaft attachment. The packed rhizotrunks were kept in boxes with water up to the height of rhizotrunks for 3 days for settlement of the puddled soil. After this settlement, the soil was 2–3 cm below the top of the rhizotrunk.

For each soil type, two extra rhizotrunks were packed to measure the water potential and moisture content of the AWD treatment during the growing period. Two tensiometers were installed at 8 cm depth permanently in each extra rhizotrunk, one in each side (root zone and bulk soil) to monitor the water potential of the AWD treatment. The readings of tensiometers were recorded every hour. In addition, a TDR probe was inserted every day at a depth of 5 cm in both the root-zone and bulk soil of these extra rhizotrunks to monitor soil moisture content during the growing period that is described next.

Rice seeds were placed on wet filter paper at 25°C for 48 h for germination. Two germinated seeds were planted in one side of each split rhizotrunk at a depth of 4 mm from the soil surface. After 7 days of planting, the seedlings were reduced to one plant per rhizotrunk by removing the weakest plant. Rhizotrunks were kept in large plastic boxes (volume of each box was 84,000 cm^3) at around a 15° angle to encourage roots to grow along the mesh between the two sides. All the plants were grown for 4 weeks. This was during the Aberdeen, UK winter and the soil rhizotrunks were kept in a tropical greenhouse with day/night temperatures of 28/24°C, light intensity 464 μmol m^{-2} s^{-1} and 11 h photoperiod. Plant height, number of leaves and tillers were also recorded during growing period.

Over the growing period, half of the rhizotrunks remained flooded and the other half had simulated AWD irrigation. AWD was applied from 10 days after transplanting. For the CF treatment, 2–3 cm standing water (above the soil level) was maintained throughout the growing cycle for 1 week before harvesting, at which point adding water ceased so that the soils dried to enable destructive harvest and X-ray CT scanning. The AWD irrigation treatment was imposed by re-watering the soil to flooded once the soil water potential reached to −15 kPa.

2.3 | Dualex data collection

The nitrogen balance index (NBI), which is good indicator of plant nitrogen status, chlorophyll, anthocyanin and flavonoid content was measured 1 week before harvesting on the fully grown second leaf from the top using a ForceA Dualex (optical leaf clip) meter (Paris, France).

2.4 | Harvesting and measurement of root parameters

At harvest, shoots were cut at the soil surface. Shoot fresh weight was measured before drying in an oven at 70°C for 72 h for shoot dry weight. The rooted and bulk side of each rhizotrunk was separated and three small (1 × 1 × 1 cm) samples from 3 cm (top), 17 cm (middle) and 25 cm (bottom) depths below the surface of each side were carefully cut out using a sharp blade. The locations on the rooted side were picked carefully to include few fine roots. On the non-rooted side of the rhizotrunk, samples were taken away from where roots were visible across the mesh on the rooted side. These samples were fixed to a petridish using a glue gun so that the soil could be handled and measurements made. The petri dishes were immediately sealed with Parafilm and stored at 4°C until testing. There was less than 96 h between sampling and measurements of the small subsamples.

Then on the remaining rooted side of the rhizotrunk, all the roots were washed using tap water over a 2 mm sieve. The cleaned root samples were placed in plastic containers with 50% ethanol and then kept in a refrigerator at 4°C until root traits was measured. The cleaned roots were placed in a glass tray filled with water to about 4 mm depth. From each sample, all the roots were spread out with tweezers to reduce overlapping and scanned with an A3 size Expression 10000XL scanner (Epson, Suwa, Japan) at 600 dots per inch (DPI). The root length, average diameter, volume, branch number and tip number for roots were determined by the root analysis software, WinRhizo Ver. 2013e (Regent Instruments, Quebec City, Canada). The roots were then dried at 70°C to measure root dry weight.

2.5 | X-ray CT imaging

The subsampled soil fixed to the petri dish was scanned using an industrial X-ray CT system (X-TEK XTH 225, Nikon Metrology, Tring, UK) with settings of 100 kV, 140 μA and 1000 ms exposure time, averaged over 3 images. The isotropic voxel size was 13 μm. Image reconstruction was performed using CT Pro 3D (Nikon Metrology, version XT 4.3.1). All images were processed using FIJI (version 2.9.0) (Schindelin et al., 2012) and VG StudioMax 2.1. The original images were 16 bit. At first images were imported to FIJI and converted to 8 bit

grayscale, followed by cropping to a region of interest (ROI) of $8 \times 8 \times 8$ mm to avoid edge effects. Then 3D Gaussian and Median filters ($1 \times 1 \times 1$ Kernel size) were applied to reduce noise and thresholding quality in the cropped images. As watering stopped a week before harvesting for AWD and CF rhizotrunks, the impact of water content during segmentation was decreased. The filtered images were used for segmenting pore space and solids using the default thresholding algorithm provided in the FIJI (version 2.9.0). This thresholding process produced 3D binary images. Subsequent image analysis was done using 3D binary images. BoneJ plugin of ImageJ was used for getting a thickness map of pore network of desired image and the pore network was linked to a histogram to obtain 3D information regarding pore size distribution using voxel-counting approach. Although our intention was to identify roots in the images as well, there was insufficient contrast for reliable detection, so they are treated as pores in our analysis. Some fine roots could be visualised, but no large roots were present in the ROIs examined, hence the difficulty in resolving roots.

2.6 | Topological properties of soil pores

Within the ROI, a range of soil pore topological properties were analysed from the 3D X-ray CT images. The macroporosity was measured as the ratio of volume of thresholded pores and total volume of the ROI. The thickness algorithm within the Particle Analyser plugin in ImageJ was used to measure the average pore diameter (Kutay et al., 2007). The BoneJ particle analyser plugin in ImageJ (Domander et al., 2021) was used to calculate the Euler's number (χ). This number is commonly used to measure connectivity of pore networks from the total number of isolated pores (N) minus the number of redundant connections (C) plus the number of completely enclosed cavities (H) (Vogel, 1997). A negative Euler number indicates percolating pores (Katuwal et al., 2015).

Three pore shape properties, circularity, roundness and aspect ratio, were determined using the Analyse Particles plugin in ImageJ. If these values are close to one it means the pores are circular in shape. On the other hand, when circularity and roundness are close to zero and aspect ratio is higher than one, it indicates that pores are elongated in shape (Norhidayah et al., 2014).

2.7 | Mechanical properties

Soil hardness and modulus of elasticity were measured on the same samples used for the X-ray CT scanning. Subsequently after X-ray CT scanning, samples were oven dried at 40°C for 72 h. One indentation measurement was performed on each soil sample using a 2 mm diameter spherical indenter fitted to a Z05 mechanical test frame (Zwick GmbH, Ulm, Germany). A 100 N load cell accurate to 0.2% was used for this test. The surface of soil was indented at a rate of 1 mm min^{-1} rate to 0.5 mm depth and then unloaded at the same speed. The loading and un-loading versus displacement curve was used to calculate soil hardness and elasticity, as described in Naveed et al. (2018).

2.8 | Hydrological properties

After the indentation test, soil hydrological properties were measured in both the root-zone and bulk soil. To obtain measurements at small-scale, a miniaturised infiltrometer device (0.36 mm radius) was used to obtain water sorptivity, ethanol sorptivity and water repellency (Hallett et al., 2003). Sorptivity is a measure of the ability of a medium to absorb or desorb liquid. Many factors such as the soil water content, structure, porosity and hydrophobicity can affect water sorptivity. To determine soil hydrophobicity, ethanol sorptivity was also measured because its nonpolar nature is not affected by the hydrophobicity of the soil. Infiltration rates of both water and ethanol were recorded from a 0.1 mg range balance at every second for 180 s. A hydraulic head of −1 mm was applied for all measurements. The constant rate of liquid flow (Q) was generally found after 20 s. From the values of water sorptivity (S_W) and ethanol sorptivity (S_E), a water repellency index, R, was calculated as described in Hallett et al. (2003). Values of $R > 1$ indicate that the soil is water repellent.

2.9 | Statistical analyses

The experiment was a 2×2 (two water regimes and two soil textures) factorial design with 4 treatment combinations. Each treatment was replicated 4 times. All the statistical analyses were performed using R (version 4.2.2) in the R Studio environment. The homogeneity of variances and normality of residuals were checked by the Bartlett and Shapiro–Wilk tests, respectively before any further statistical tests. Two-way ANOVA was performed for above ground parameters and root characteristics, with water regimes and soil textures as the two factors. All the mechanical, hydrological and pore topological properties were assessed by three-way ANOVA with water regime (AWD and CF), soil texture (sandy loam and silty clay loam) and side (root-zone and bulk) as three factors and their interactions were also assessed. A least significant

difference (LSD) test was used for post hoc analysis at $p < 0.05$.

3 | RESULTS

3.1 | Above ground plant properties

The shoot dry weights were significantly affected by water regimes as well as soil textures, with AWD 22% less than CF (Table 1) and 64% greater in silty clay loam than sandy loam soils (Table 1). There was no significant interaction on shoot dry weight between water regimes and soil textures.

Plant height also varied between water regimes and soil textures. Plants were 10% taller under CF than AWD irrigation treatment and 11% taller in silty clay loam compared to sandy loam soil (Table 1). There was an interaction between water regimes and soil textures. The negative impact of AWD on plant height was only apparent in the sandy loam.

The number of leaves did not differ between water regimes, but it was significantly less in sandy loam than in silty clay loam soils (Table 1). Similarly, tiller number was also not impacted by the water regimes. However, silty clay loam soil had 80% more tiller number compared to sandy loam soil (Table 1).

The root-shoot ratio was 37% greater for the AWD treatment than the CF treatment. Additionally, there was about 22% greater root: shoot ratio in sandy loam soil in contrast to silty clay loam soil (Table 2).

The plants treated with CF irrigation had 18% more NBI and 10% greater chlorophyll content than plants grown in AWD (Table 1). On the other hand, the plants grown under silty clay loam soil had more NBI and chlorophyll content (Table 1) in comparison with sandy loam

TABLE 1 Different plant parameters and Dualex data of Black Gora grown under different water regime and soil texture treatments.

Water regime	Soil texture	Plant height (cm)	Number of tiller	Number of leaves	Shoot dry weight (g)	NBI	Chlorophyll ($\mu g\ cm^{-2}$)	Anthocyanin ($\mu g\ cm^{-2}$)
AWD	Silty clay loam	80.66 (1.72)	1.67 (0.21)	7.50 (0.67)	0.89 (0.04)	24.75 (1.33)	23.53 (0.79)	0.372 (0.002)
	Sandy loam	68.83 (0.91)	1.00 (0.00)	5.00 (0.00)	0.53 (0.02)	15.56 (0.64)	15.95 (0.68)	0.379 (0.003)
CF	Silty clay loam	83.75 (2.39)	2.00 (0.00)	8.00 (0.41)	1.13 (0.11)	28.07 (1.92)	24.52 (0.97)	0.340 (0.008)
	Sandy loam	80.50 (1.55)	1.00 (0.00)	5.00 (0.00)	0.69 (0.03)	19.5 (1.92)	18.72 (0.75)	0.361 (0.003)
Analysis of variance								
Water regime (W)		19.71***	NS	NS	13.35**	6.55*	5.33*	26.38***
Texture (T)		26.63***	38.40***	37.63***	51.71***	41.42***	73.82***	11.47**
W × T		6.67*	NS	NS	NS	NS	NS	NS

Note: Numbers in the brackets are standard error of the mean. For the analysis of variance, values reported are the *f*-values and different asterisk indicating the level of significance at different probability. NS means non-significant at the $p = 0.05$ level.
***$p < 0.001$; **$p < 0.01$; *$p < 0.05$.

TABLE 2 Different root parameters of Black Gora rice grown under different water regime and soil texture treatments.

Water regime	Soil texture	Root dry weight (g)	Root-shoot ratio	Root length (cm)	Root surface area (cm^2)	Root diameter (mm)	Root volume (cm^3)	Root tips
AWD	Silty clay loam	0.41 (0.03)	0.45 (0.02)	4980.62 (243.45)	380.72 (19.29)	0.24 (0.003)	2.31 (0.13)	42,485 (1732)
	Sandy loam	0.28 (0.02)	0.52 (0.01)	7067.16 (342.56)	470.26 (26.14)	0.21 (0.004)	2.49 (0.16)	77,350 (2774)
CF	Silty clay loam	0.35 (0.06)	0.30 (0.02)	4355.48 (607.33)	362.44 (53.95)	0.26 (0.005)	2.40 (0.38)	30,197 (3874)
	Sandy loam	0.29 (0.03)	0.41 (0.03)	6754.11 (534.63)	492.39 (45.29)	0.23 (0.005)	2.86 (0.31)	79,392 (5923)
Analysis of variance								
Water regime (W)		NS	35.23***	NS	NS	19.23***	NS	NS
Texture (T)		7.96*	15.43**	29.73***	9.79**	50.23***	NS	142.96***
W × T		NS	NS	NS	NS	NS	NS	NS

Note: Numbers in the brackets are standard error of the mean. For analysis of variance, values reported are the *f*-values and different asterisks indicating the level of significance at different probabilities. NS means non-significant at the $p = 0.05$ level.
***$p < 0.001$; **$p < 0.01$; *$p < 0.05$.

soil. Similarly, anthocyanin content was higher for plants grown in AWD than CF treatment. It was greater for plants grown in sandy loam soil compared to silty clay loam soil (Table 1). There were no influences of water regimes and soil textures on flavonoid content (data not shown).

3.2 | Below ground plant parameters

The water regime had no influence on root dry weight, root length, root surface area or number of root tips (Table 2). There were impacts on these properties by soil texture. Root dry weight was 35% greater for the plants grown in silty clay loam soil than sandy loam soil. Root length and tips were consistently greater in sandy loam soil when compared with silty clay loam soil (Table 2). An interaction effect between water regimes and soil textures on root length was not observed. Root surface area increased by 28% for plants grown in sandy loam soil compared to silty loam soil (Table 2).

Water regime did affect the root diameter, which was thicker in CF in comparison with AWD. Sandy loam soil resulted in a 13% smaller root diameter than silty clay loam (Table 2).

3.3 | Soil pore structure

From X-ray CT images, compared to CF, AWD had greater macroporosity and number of pores across the rhizotrunk. Although average pore area was greater for AWD in the top and middle, it was affected by water regimes in the bottom of rhizotrunk. Macroporosity and number of pores were significantly greater for silty clay loam soil compared to sandy loam soil in the top and middle of the rhizotrunk (Figure 2 and Table 3). However, average pore size was less for silty clay loam soil in the top and middle. Additionally, a decrease of 35% macroporosity was found in silty clay loam soil compared to sandy loam soil at the bottom (Figure 2). On the other hand, the number of pores and average pore area were not affected by the soil textures in the bottom of the rhizotrunk. The presence of roots significantly increased the macroporosity, number of pores and average pore area throughout the soil profile of the rhizotrunk (Figure 2 and Table 3).

Pores were wider for soil under AWD compared to CF in the top of the rhizotrunk. In contrast, water regimes had no effect on pore diameter in the middle and bottom soil. Additionally, a 36% thinner pore diameter was observed in the silty clay loam compared to sandy loam soil in the top (Figure 4). Pore diameter was similar for both silty clay loam and sandy loam soil in middle and bottom (Table S1). The presence of roots increased pore diameter by 60%, 37% and 75% in the top, middle and bottom soil, respectively (Figure 4).

There were no effects of water regimes on the Euler number for both top and middle soil depths. On the contrary, pores were more connected in AWD than CF in the bottom of the rhizotrunk (Table 3). There was no impact of soil texture on Euler number in the top and middle of the rhizotrunks (Table 3), but the Euler number suggested that pores were highly connected in sandy loam soil in the bottom depth (Tables S1 and 3). Euler number did not differ between bulk soil and the root-zone in both the top and middle of the rhizotrunk (Table S1). However, Euler number was negative for the root-zone in the bottom of the rhizotrunk, which means the pores were more connected (Table 3).
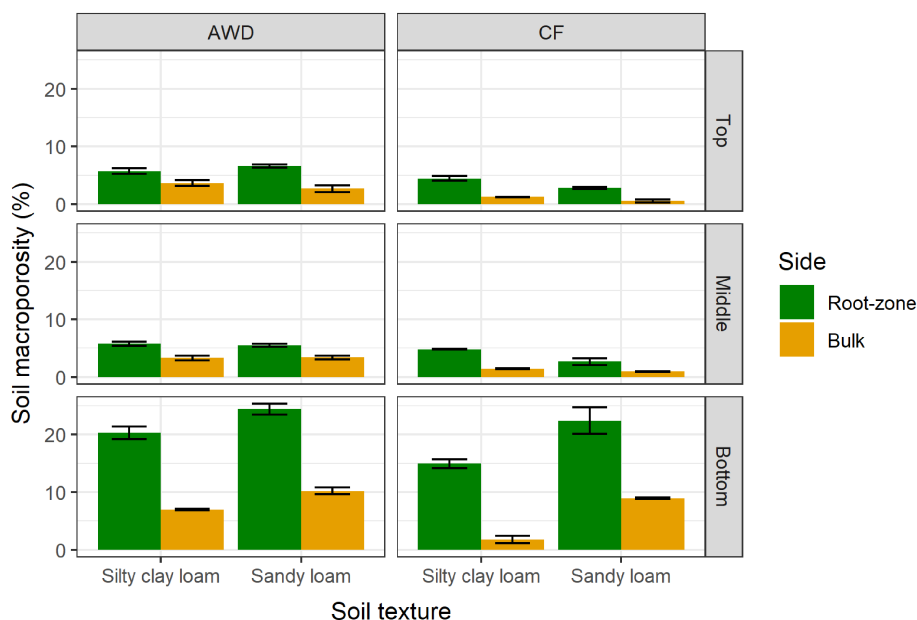

FIGURE 2 Soil macroporosity in the root-zone and bulk soil under alternate wetting and drying (AWD) and continuous flooding (CF) treatments in different soil depths calculated from X-ray CT images. Error bars denote the standard error of the mean ($n = 3$).

TABLE 3 Euler number and different pore characteristics of the root-zone and bulk soil under AWD and CF treatments in different soil depths.

Depth	Water regime	Side	Soil texture	Pore number	Average pore area (mm^2)	Pore circularity (%)	Pore roundness (%)	Pore aspect ratio (%)	Euler's number
Top	AWD	Bulk	Silty clay loam	29.7 (4.7)	0.054 (0.007)	0.81 (0.007)	0.61 (0.008)	2.00 (0.015)	1042 (667)
			Sandy loam	15.0 (1.1)	0.245 (0.056)	0.85 (0.011)	0.67 (0.011)	1.85 (0.162)	3223 (1304)
		Root-zone	Silty clay loam	38.4 (0.5)	0.179 (0.108)	0.80 (0.011)	0.59 (0.016)	2.08 (0.098)	1796 (235)
			Sandy loam	32.7 (1.5)	0.690 (0.125)	0.82 (0.017)	0.62 (0.011)	2.05 (0.141)	2096 (157)
	CF	Bulk	Silty clay loam	12.1 (0.9)	0.041 (0.017)	0.84 (0.030)	0.63 (0.031)	1.92 (0.052)	239 (49)
			Sandy loam	10.3 (0.7)	0.013 (0.005)	0.83 (0.016)	0.64 (0.020)	1.92 (0.003)	2980 (2546)
		Root-zone	Silty clay loam	22.7 (3.7)	0.157 (0.055)	0.79 (0.015)	0.59 (0.013)	2.17 (0.120)	1100 (183)
			Sandy loam	23.3 (0.9)	0.004 (0.008)	0.77 (0.012)	0.59 (0.010)	2.04 (0.063)	1376 (461)
Middle	AWD	Bulk	Silty clay loam	15.5 (0.5)	0.069 (0.003)	0.84 (0.011)	0.64 (0.006)	1.81 (0.029)	1110 (164)
			Sandy loam	10.6 (1.3)	0.236 (0.068)	0.71 (0.011)	0.55 (0.015)	1.83 (0.114)	673 (88)
		Root-zone	Silty clay loam	46.0 (4.0)	0.229 (0.015)	0.76 (0.011)	0.59 (0.012)	2.04 (0.064)	1084 (502)
			Sandy loam	28.3 (2.4)	0.374 (0.041)	0.77 (0.006)	0.59 (0.010)	2.13 (0.065)	845 (59)
	CF	Bulk	Silty clay loam	9.0 (1.0)	0.058 (0.018)	0.85 (0.010)	0.64 (0.012)	2.00 (0.215)	700 (500)
			Sandy loam	6.5 (1.5)	0.188 (0.037)	0.71 (0.021)	0.53 (0.017)	2.03 (0.248)	943 (126)
		Root-zone	Silty clay loam	19.5 (1.5)	0.128 (0.007)	0.74 (0.012)	0.55 (0.001)	2.30 (0.120)	548 (66)
			Sandy loam	15.0 (3.0)	0.316 (0.151)	0.79 (0.007)	0.61 (0.004)	1.98 (0.033)	1149 (102)
Bottom	AWD	Bulk	Silty clay loam	159.6 (37.6)	0.068 (0.038)	0.81 (0.003)	0.63 (0.001)	1.80 (0.014)	5588 (2400)
			Sandy loam	195.0 (7.5)	0.022 (0.001)	0.83 (0.011)	0.64 (0.015)	1.73 (0.071)	5524 (438)
		Root-zone	Silty clay loam	173.9 (36.0)	0.072 (0.012)	0.70 (0.024)	0.57 (0.027)	2.06 (0.090)	−1938 (1419)
			Sandy loam	220.7 (6.9)	0.070 (0.007)	0.74 (0.006)	0.61 (0.006)	1.83 (0.010)	−12,951 (3839)
	CF	Bulk	Silty clay loam	115.4 (5.4)	0.012 (0.004)	0.88 (0.009)	0.67 (0.012)	1.69 (0.017)	9228 (958)
			Sandy loam	77.5 (2.5)	0.008 (0.004)	0.79 (0.010)	0.61 (0.010)	1.76 (0.027)	7732 (953)
		Root-zone	Silty clay loam	161.9 (31.9)	0.031 (0.012)	0.75 (0.009)	0.60 (0.009)	1.86 (0.032)	−1026 (911)
			Sandy loam	184.0 (4.0)	0.096 (0.061)	0.72 (0.012)	0.59 (0.011)	2.07 (0.162)	−3381 (1396)

Note: Numbers in the brackets are standard error of the mean.

Pore shape was not affected by the water regime or soil texture. However, there were significant differences of pore shape observed between the bulk soil and the root-zone throughout the depth of soil. The root-zone had less circular pores compared to bulk soil, especially in the top and bottom of the rhizotrunk (Table 3).

3.4 | Mechanical properties

Soil hardness was not affected significantly by the AWD and CF treatments at different depths (Figure 5). Soil texture had erratic impacts on soil hardness depending on the depth of measurement (Table S1). The soil hardness increased by 20% in the top and 53% in the middle in the root-zone compared to bulk soil, but it was less in the root-zone at the bottom of the rhizotrunk (Figure 5).

Similar to hardness, water regime had no impact on the soil modulus of elasticity at any depths. Although silty clay loam soil had 41% greater modulus of elasticity in the bottom than sandy loam soil (Figure 6), at other depths there were no differences (Figure 6). In the middle of the rhizotrunk, texture and the root-zone interacted to affect the modulus of elasticity (Figure 6 and Table S1). Moreover, the root-zone soil had 31% greater elastic modulus at the top and 42% greater elastic modulus at the middle compared to bulk soil, while there was no difference of modulus of elasticity for the root-zone and bulk soil at the bottom (Figure 6).

3.5 | Hydrological properties

Water sorptivity was similar for AWD and CF treated soil at the top, whereas there was an interaction between

FIGURE 3 Greyscale images of puddled layer showing macropores of the root-zone and bulk (silty clay loam & sandy loam) soil under different water regimes. Annotation highlights the presence of macropores.
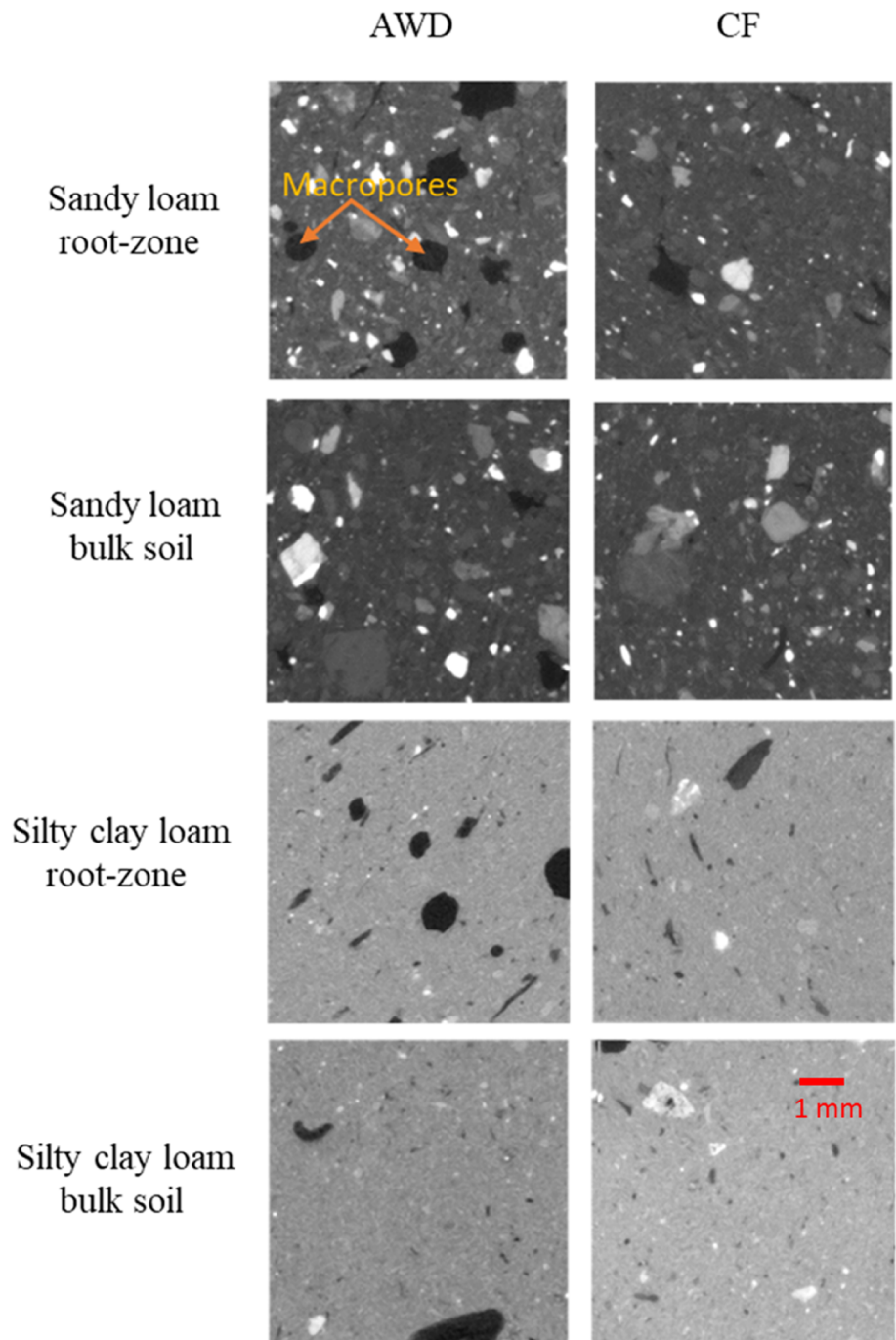
water regime and the side of the rhizotrunk, being greatest in the top for the root-zone under AWD (Figure 7). Furthermore, AWD had 57% faster water sorptivity than soil under CF in the middle depth, but there were no influences of water regimes at the bottom depth. In contrast, water sorptivity was slower at all depths for silty clay loam compared to sandy loam soils (Figure 7). On the other hand, water sorptivity was 36% and 51% greater in the root-zone compared to that in the bulk soil at the top and bottom, respectively, but not in the middle (Figure 7).

The soil under AWD had significantly less ethanol sorptivity than soil under CF treatment at the top and bottom of the rhizotrunk, but not the middle (Figure 8). On the other hand, sandy loam soil had 89% greater ethanol sorptivity in the top and 75% higher ethanol sorptivity in the middle compared to silty clay loam soil (Figure 8). Conversely, there was no effect of soil texture on the ethanol sorptivity at the bottom (Table S1). Ethanol sorptivity was 34% greater in the top and 23% greater in the middle for the root-zone soil compared to bulk soil, but not different at the bottom (Figure 8).
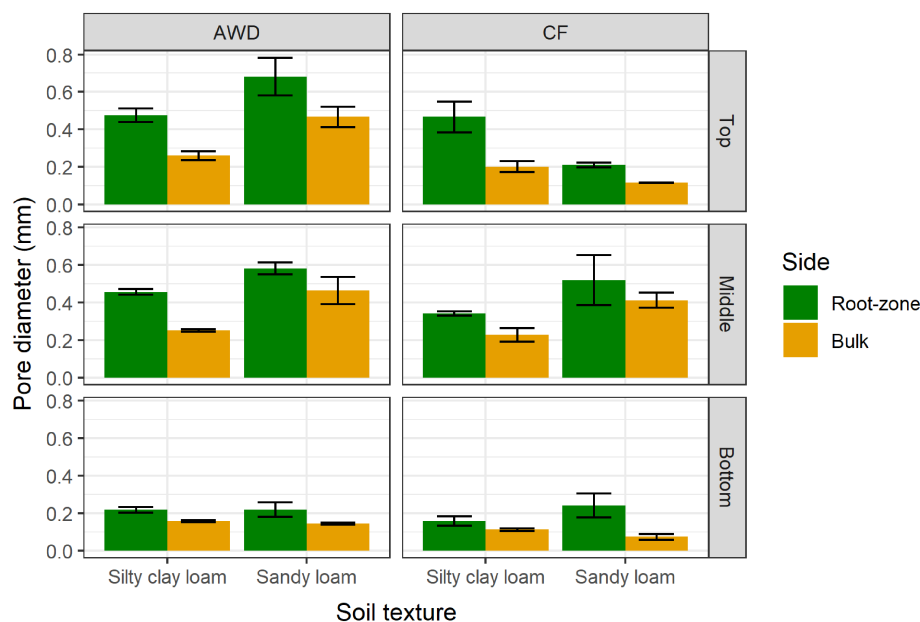
FIGURE 4   Diameter of the pores in the root-zone and bulk soil under alternate wetting and drying (AWD) and continuous flooding (CF) treatments in different soil depths calculated from X-ray CT images. Error bars denote the standard error of the mean ($n = 3$).
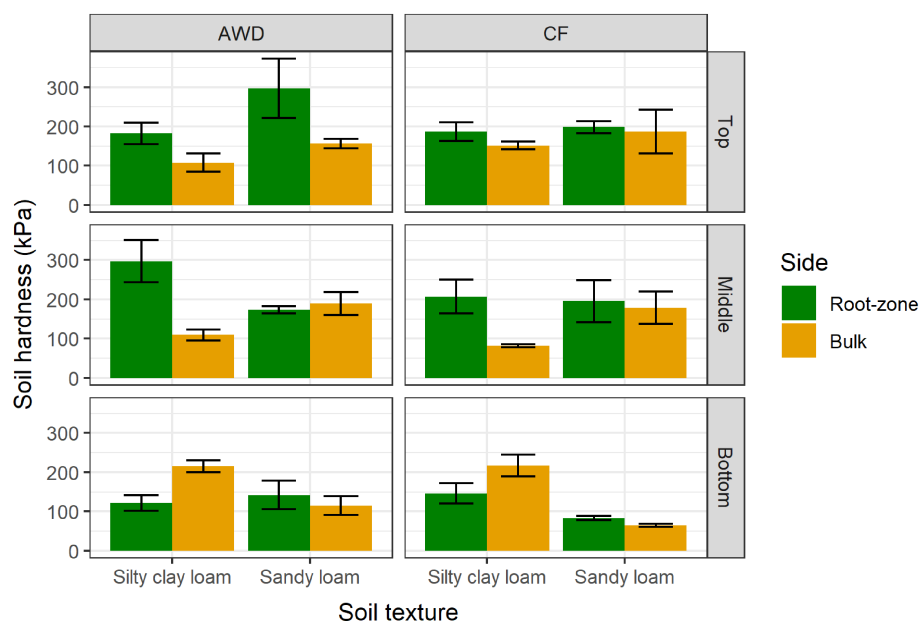
FIGURE 5   Soil hardness in the root-zone and bulk soil under alternate wetting and drying (AWD) and continuous flooding (CF) treatments in different soil depths measured by an indenter test using a standard loading frame. Error bars denote the standard error of the mean ($n = 4$).

There were no significant effects of water regimes, soil textures and presence of roots on the water repellency at the top of the rhizotrunk (Table S1 and Figure 9). However, there was an interaction effect between water regimes, rhizotrunk side and soil textures in the soil at the top. The silty clay loam root-zone under CF had greatest water repellency compared to other treatment combinations. However, the root-zone soil was more repellent than bulk soil in the middle (Figure 9). Additionally, soil under AWD was less water repellent in the middle and bottom of the rhizotrunk. On the other hand, there was a great impact of soil textures on the water repellency of the bottom soil. Silty clay loam was

more repellent compared to sandy loam soil at the bottom (Table S1 & Figure 9).

4 | DISCUSSION

Combined measurements of the pore structure, mechanical and hydrological properties of soil have demonstrated large impacts of both plant roots and AWD compared to CF irrigation regimes on the root-zone soil. This combination of imaging and direct hydromechanical measurements goes beyond previous studies that found roots to induce soil structural and

FIGURE 6 Soil modulus of elasticity in the root-zone and bulk soil under alternate wetting and drying (AWD) and continuous flooding (CF) treatments in different soil depths measured by indenter test using a standard loading frame. Error bars denote the standard error of the mean ($n = 4$).
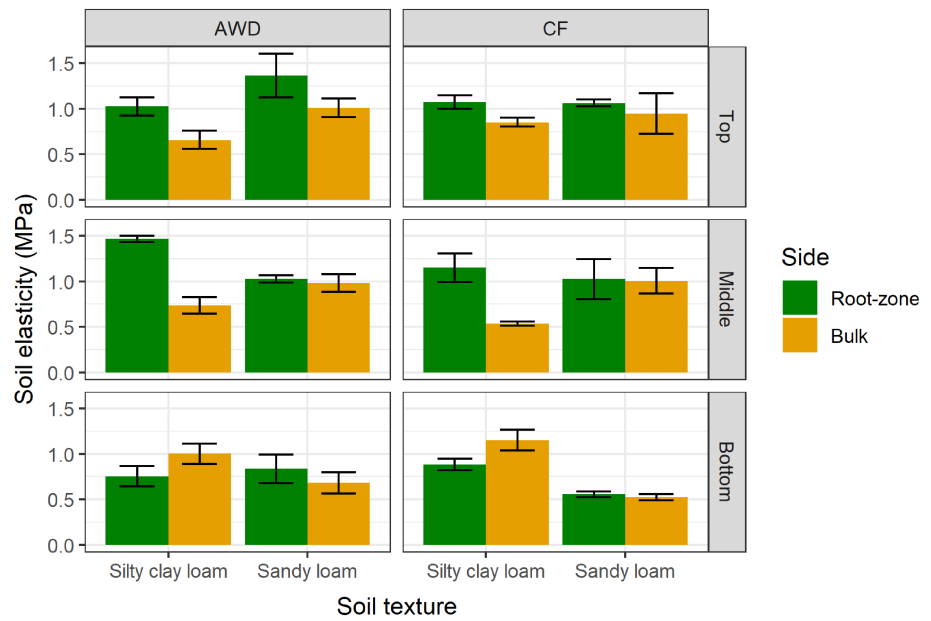
FIGURE 7 Water sorptivity in the root-zone and bulk soil under alternate wetting and drying (AWD) and continuous flooding (CF) treatments in different soil depths measured by miniaturised infiltrometer method. Error bars denote the standard error of the mean ($n = 4$).
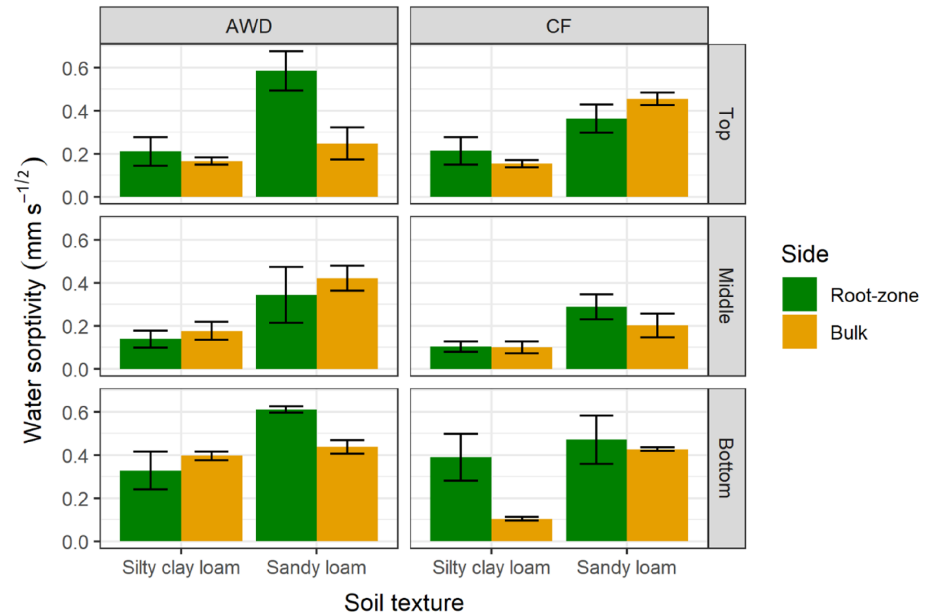

hydrological changes (Carminati et al., 2013; Gregory, 2006; Hallett et al., 2009). It is also the first study using small-scale measurements to explore the impacts of rice roots and AWD on physical properties of the root–soil interface. Our setup sampled along a zone of concentrated root growth, so the impacts are likely indicative of rhizosphere properties.

Overall, the results suggest that AWD compared to CF could promote soil structure development in the root zone that transmits water more effectively through its larger and better-connected pore system. Our findings also showed that pores in the root-zone were less circular than bulk soil, which is very important for rice root growth from the surface to the subsoil (Islam et al., 2021). These changes were expected and likely due to soil shrinkage under AWD that would be exacerbated by root water uptake and exudation.

4.1 | Impacts of AWD on the plant vegetative growth

Water management played a significant role in the vegetative growth of the rice plants. The plants grown under AWD were significantly shorter and had lower shoot dry weight in relation to CF (Table 1), possibly due to slight water stress in AWD. This agrees with Liao et al. (2020) who conducted a pot experiment and found that plant height reduces under AWD compared to CF. However, there was no significant variation of the number of tillers and leaves between the AWD and CF treatments. This is consistent with the findings of Bwire et al. (2022) who found in a greenhouse study that water regimes had no effects on the number of tillers. Additionally, AWD is
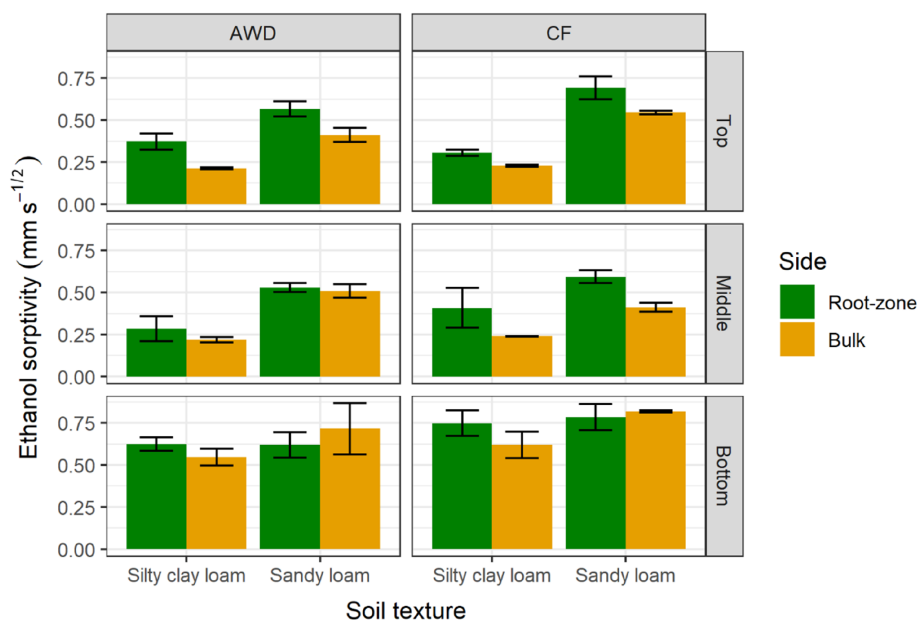
FIGURE 8 Ethanol sorptivity in the root-zone and bulk soil under alternate wetting and drying (AWD) and continuous flooding (CF) treatments in different soil depths measured by miniaturised infiltrometer method. Error bars denote the standard error of the mean ($n = 4$).
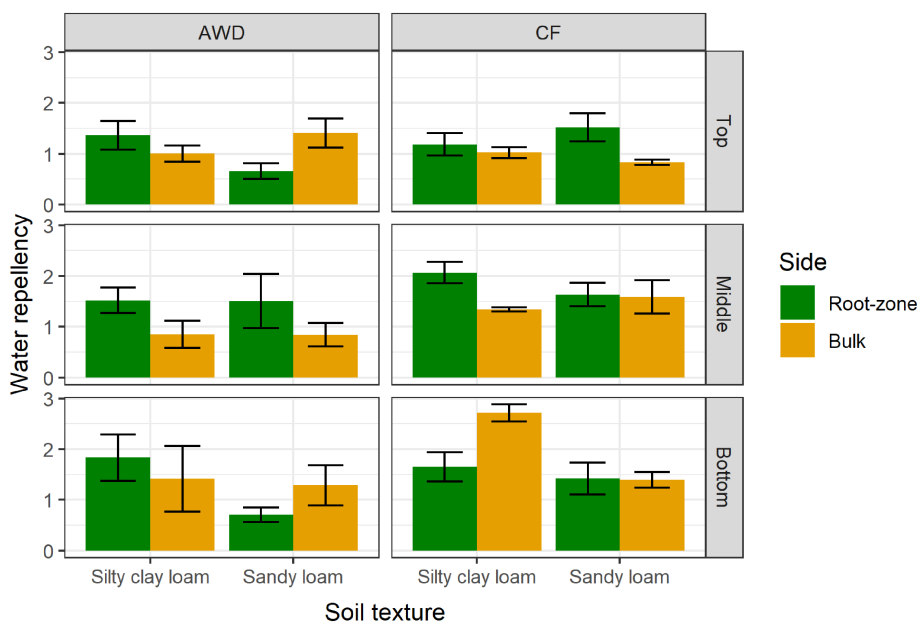
FIGURE 9 Water repellency in the root-zone and bulk soil under alternate wetting and drying (AWD) and continuous flooding (CF) treatments in different soil depths measured by miniaturised infiltrometer method. Error bars denote the standard error of the mean ($n = 4$).

beneficial because it reduces the redundant vegetative growth which leads to increased root activities, healthy canopy structure and higher yield (Yang & Zhang, 2010). There are conflicting data from field studies, such as a 12%–15% increase in shoot mass recorded in AWD compared to CF during harvesting (Norton et al., 2017). In that study the number of tillers was double in AWD compared to CF. This contradictory finding might be due to differences in growth stage because they measured plant growth parameters at harvest (ripening), but our results are only at 4 weeks of growth. Additionally, water potential is very important for determining the impacts of AWD on the growth and yield of rice (Carrijo et al., 2016), which might be different from our study

because we maintained a specific water potential (-15 kPa) for the AWD treatment.

4.2 | Influences of AWD and rice root on soil pores characteristics

Many AWD studies have observed cracks that develop during the drying phase (Bottinelli et al., 2016; Lu et al., 2000; Maruyama, 1997) due to shrinking and swelling of soil (Passioura, 1991). This larger-scale process will affect subsequent irrigation water movement, but we also found like Fang et al. (2018) that AWD increased macropore formation in the root-zone, likely driving the

improved hydraulic properties that were measured. As found in our research at small-scale close to roots, some field studies have reported that AWD enhances the formation of soil macroporosity (Pires et al., 2007; Pires et al., 2008). Our result also showed that the root-zone had greater macroporosity (assessed using high resolution X-ray CT image analysis for small samples) compared to bulk soil (Figures 2 and 3), agreeing with Helliwell et al. (2017) who explored various types of soils. Similarly, a field study with 12 crop species showed that coarse root systems increased soil macroporosity by 30% (Bodner et al., 2014).This increasing porosity in the root-zone was likely due to the combined influence of root exudates and increased microbial activities intensifying soil aggregation (Helliwell et al., 2014). Another possible reason for greater porosity in the root-zone might be the rearrangement of soil particles or aggregates because of the forces created by the root growth mechanism in the soil (Mitchell & Soga, 2005). On the contrary, our results contradict the findings of Aravena et al. (2011) who showed using X-ray CT that there was a 8%–12% reduction of porosity in the sunflower root zone due to exerted compression of soil from root expansion. However, their study explored soil directly adjacent to one large root, whereas our work on rice used a sample likely affect by several fibrous roots that were interacting.

We also found that the root-zone soil had a greater number and bigger pores than bulk soil. Sources of these pores could be growing roots generating cracks (Fang et al., 2018) and the creation secondary lateral pore channels by the reorientation of soil particles during shrinking and swelling cycles (Horn & Dexter, 1989).

Interestingly, our results also showed that the shape of pores in the root-zone was less circular and rounded compared to bulk soil. This also suggests the creation of elongated cracks from roots growing through the soil (Nong et al., 2023). At the same time, extraction of water by the plant roots would cause shrinkage of the soil (Materechera et al., 1992), leading to cracking (Yoshida & Hallett, 2008). The better pore connectivity in the root-zone and in AWD that we found could be attributed directly to the greater macroporosity, especially cracking discussed previously. In addition, pore connectivity is a function of pore size (Vogel, 1997), which was also larger in the AWD root-zone. Using higher resolution imaging of root-zone soil with synchrotron imaging, Koebernick et al. (2017) found greater pore connectivity in the root-zone than that in the bulk soil for barley. Cracking would be expected to be greater in silty loam textured soils due the amount of fine particles (Yoshida & Hallett, 2008), creating more connected pores that are found for this soil in the root-zone and under AWD (Table 2) where hydraulic stresses shrinking and swelling the soil would be greatest (Marin et al., 2022).

4.3 | Influences of AWD and rice root on soil mechanical characteristics

Although the root-zone had greater hardness and elasticity than bulk soil, AWD had no impact compared to CF irrigation. Our findings are supported by the results of a controlled environment study conducted by Naveed et al. (2018) who found that barley and maize root significantly increased soil hardness and elasticity in sandy loam and clay loam soil. However, this study had much different soil structure (sieved soil) compared to our soil (puddled). For rice under paddy conditions, plant roots have been found to increase the soil strength and shear resistance measured at larger scale (Willatt & Sulistyaningsih, 1990). At the scale of the root–soil interface, soil compression by plant roots, exudation and soil aggregation under drying stresses likely drive the mechanical changes we observed. Even though the root-soil interface had greater macroporosity, it was still harder and had a larger elastic modulus than that of the bulk soil. There could be potential to select rice for root surface traits such as root hairs for beneficial impacts to rhizosphere mechanical properties. In barley, Marin et al. (2022) found a hairy root genotype reduced soil hardness (by 50%) and elasticity (by 36%) compared to a hairless mutant in silty loam soil. Potential exists to explore this more for rice, given our genetic understanding of root hair traits for this species (Hanlon et al., 2023).

Our results also showed that the presence of rice roots decreased soil hardness in the sieved soil layer (bottom) in contrast to the puddled layer. Therefore, initial soil structure is important to predict the root-induced mechanical changes alongside others factors such as soil texture, drying cycles and plant species (Helliwell et al., 2019).

4.4 | Influences of AWD and rice root on soil hydrological characteristics

The rate that the root-zone absorbs water was greater under AWD compared to the CF root-zone for the top and bottom soil in the rhizotrunk (Figure 7). This improved water sorptivity aligns with the greater macroporosity and pore connectivity found in the root-zone (Figures 2, 3 and Table 3). Countering increased water sorptivity in the root-zone could be an increase in water repellency, as has been observed in several studies (Benard et al., 2019; Hallett et al., 2009; Naveed et al., 2018). We also found that soil in the root-zone had greater water repellency than bulk soil, but that levels were quite low and not enough to cause a large decrease to water sorptivity. Irrigation with AWD resulted in less water repellent soil in the middle and bottom of the rhizotrunk compared to

CF treatment, but topsoil was not affected by the water regimes. This was surprising as the top is the hydrologically dynamic zone, whereas the middle and bottom soil remains saturated in AWD (Belder et al., 2004). There are interacting impacts from rhizodeposition and pore structure modification by the plant roots depends on soil conditions (Lucas et al., 2019; Phalempin et al., 2021) that affect water repellency, so disentangling the trends we observed is difficult.

This was a controlled greenhouse experiment limited to young plants. As soils in the field have more complex pore structures and hydroclimatic conditions between AWD and CF could vary more than in our controlled approach, future research should be conducted with temporal sampling to harvest in the field. Such research could also extend to exploring contrasting root architectural and root-surface traits (Hallett et al., 2022) of rice. Furthermore, to obtain high resolution images where roots and the root–soil interface could be resolved, we used very small samples for imaging to calculate different topological properties. The experiment could be conducted across a number of scales to learn more about whole root-zone processes.

5 | CONCLUSIONS

Our research showed that AWD has great impact on the modifications of soil structure by rice roots. Therefore, irrigation practices could be a good option for improving the resource capture from the soil at small scale for sustainable rice production. To the best of our knowledge this is the first study at small scale that quantified hydromechanical processes directly in paddy soil. Rhizosphere scale soil stabilization by plant roots is well observed for the major crops wheat, maize and barley. Our results also showed that rice roots modify soil mechanical and hydrological properties, which can have direct impact on the growth and development of plants. The effects of soil structural modification can be greater in paddy soil as it starts as structureless puddled soil. With AWD, improved rhizosphere physical conditions could be one driving factor that has a potential to improve production sustainability.

AUTHOR CONTRIBUTIONS

Md. Dhin Islam: conceptualization; methodology; formal analysis and visualization; funding acquisition and writing original draft. Adam H. Price: conceptualization; investigation; methodology; review and editing and supervision. Paul D. Hallett: conceptualization; investigation; methodology; review and editing and supervision.

CONFLICT OF INTEREST STATEMENT

The authors declare that the research was conducted in the absence of any personal, commercial or financial relationships that could have appeared as a potential conflict of interest.

DATA AVAILABILITY STATEMENT

Data files and images are available on request to the corresponding author.

ORCID

Md. Dhin Islam https://orcid.org/0000-0002-2202-2118

REFERENCES

Aravena, J. E., Berli, M., Ghezzehei, T. A., & Tyler, S. W. (2011). Effects of root-induced compaction on rhizosphere hydraulic properties–X-ray microtomography imaging and numerical simulations. *Environmental Science & Technology*, *45*, 425–431. https://doi.org/10.1021/es102566j/suppl_file/es102566j_si_001.pdf

Belder, P., Bouman, B. A. M., Cabangon, R., Guoan, L., Quilang, E. J. P., Yuanhua, L., Spiertz, J. H. J., & Tuong, T. P. (2004). Effect of water-saving irrigation on rice yield and water use in typical lowland conditions in Asia. *Agricultural Water Management*, *65*, 193–210. https://doi.org/10.1016/j.agwat.2003.09.002

Benard, P., Zarebanadkouki, M., & Carminati, A. (2019). Physics and hydraulics of the rhizosphere network. *Journal of Plant Nutrition and Soil Science*, *182*, 5–8. https://doi.org/10.1002/JPLN.201800042

Berli, M., Carminati, A., Ghezzehei, T. A., & Or, D. (2008). Evolution of unsaturated hydraulic conductivity of aggregated soils due to compressive forces. *Water Resources Research*, *44*, W00C09. https://doi.org/10.1029/2007wr006501

Bodner, G., Leitner, D., & Kaul, H. P. (2014). Coarse and fine root plants affect pore size distributions differently. *Plant and Soil*, *380*, 133–151. https://doi.org/10.1007/S11104-014-2079-8/figures/7

Bottinelli, N., Zhou, H., Boivin, P., Zhang, Z. B., Jouquet, P., Hartmann, C., & Peng, X. (2016). Macropores generated during shrinkage in two paddy soils using X-ray micro-computed tomography. *Geoderma*, *265*, 78–86. https://doi.org/10.1016/j.geoderma.2015.11.011

Bouman, B. (2009). How much water does rice use. *Rice Today*, *8*, 28–29.

Bouman, B. A. M., & Tuong, T. P. (2001). Field water management to save water and increase its productivity in irrigated lowland rice. *Agricultural Water Management*, *49*, 11–30. https://doi.org/10.1016/S0378-3774(00)00128-1

Bruand, A., Cousin, I., Nicoullaud, B., Duval, O., & Bégon, J. C. (1996). Backscattered electron scanning images of soil porosity for analyzing soil compaction around roots. *Soil Science Society of America Journal*, *60*, 895–901. https://doi.org/10.2136/sssaj1996.03615995006000030031x

Bwire, D., Saito, H., Mugisha, M., & Nabunya, V. (2022). Water productivity and harvest index response of paddy rice with alternate wetting and drying practice for adaptation to climate change. *Water*, *14*, 3368. https://doi.org/10.3390/w14213368

Carminati, A., Kaestner, A., Lehmann, P., & Flühler, H. (2008). Unsaturated water flow across soil aggregate contacts. *Advances in Water Resources*, *31*, 1221–1232. https://doi.org/10.1016/j.advwatres.2008.01.008

Carminati, A., Moradi, A. B., Vetterlein, D., Vontobel, P., Lehmann, E., Weller, U., Vogel, H. J., & Oswald, S. E. (2010). Dynamics of soil water content in the rhizosphere. *Plant and Soil*, *332*, 163–176. https://doi.org/10.1007/s11104-010-0283-8

Carminati, A., Vetterlein, D., Koebernick, N., Blaser, S., Weller, U., & Vogel, H. J. (2013). Do roots mind the gap? *Plant and Soil*, *367*, 651–661. https://doi.org/10.1007/S11104-012-1496-9/figures/9

Carrijo, D. R., Lundy, M. E., & Linquist, B. A. (2016). Rice yields and water use under alternate wetting and drying irrigation: A meta-analysis. *Field Crops Research*, *203*, 173–180. https://doi.org/10.1016/j.fcr.2016.12.002

Chidthaisong, A., Cha-un, N., Rossopa, B., Buddaboon, C., Kunuthai, C., Sriphirom, P., Towprayoon, S., Tokida, T., Padre, A. T., & Minamikawa, K. (2018). Evaluating the effects of alternate wetting and drying (AWD) on methane and nitrous oxide emissions from a paddy field in Thailand. *Soil Science & Plant Nutrition*, *64*, 31–38. https://doi.org/10.1080/00380768.2017.1399044

Cooper, L. J., Daly, K. R., Hallett, P. D., Koebernick, N., George, T. S., & Roose, T. (2018). The effect of root exudates on rhizosphere water dynamics. *Proceedings of the Royal Society A: Mathematical, Physical and Engineering Sciences*, *474*, 20180149. https://doi.org/10.1098/RSPA.2018.0149

Cui, J., & Holden, N. M. (2015). The relationship between soil microbial activity and microbial biomass, soil structure and grassland management. *Soil and Tillage Research*, *146*, 32–38. https://doi.org/10.1016/J.STILL.2014.07.005

Dexter, A. R. (1987). Compression of soil around roots. *Plant and Soil*, *97*, 401–406.

Domander, R., Felder, A. A., & Doube, M. (2021). BoneJ2–refactoring established research software version 2; peer review: 3. *Wellcome Open Research*, *6*, 37. https://doi.org/10.12688/wellcomeopenres.16619.2

Fang, H., Zhou, H., Norton, G. J., Price, A. H., Raffan, A. C., Mooney, S. J., Peng, X., & Hallett, P. D. (2018). Interaction between contrasting rice genotypes and soil physical conditions induced by hydraulic stresses typical of alternate wetting and drying irrigation of soil. *Plant and Soil*, *430*, 233–243. https://doi.org/10.1007/s11104-018-3715-5

Gee, G. W., & Bauder, J. W. (1986). Particle size analysis. In *Methods of Soil Analysis, Part 1, Physical and Mineralogical Methods*. Agronomy Monograph No. 9 (2nd ed.). Soil Science Society of America.

Gregory, P. J. (2006). Roots, rhizosphere and soil: The route to a better understanding of soil science? *European Journal of Soil Science*, *57*, 2–12. https://doi.org/10.1111/J.1365-2389.2005.00778.X

Hallett, P. D., Feeney, D. S., Bengough, A. G., Rillig, M. C., Scrimgeour, C. M., & Young, I. M. (2009). Disentangling the impact of AM fungi versus roots on soil structure and water transport. *Plant and Soil*, *314*, 183–196. https://doi.org/10.1007/S11104-008-9717-y/figures/6

Hallett, P. D., Gordon, D. C., & Bengough, A. G. (2003). Plant influence on rhizosphere hydraulic properties: Direct measurements using a miniaturized infiltrometer. *The New Phytologist*, *157*, 597–603. https://doi.org/10.1046/j.1469-8137.2003.00690.x

Hallett, P. D., Marin, M., Bending, G. D., George, T. S., Collins, C. D., & Otten, W. (2022). Building soil sustainability from root–soil interface traits. *Trends in Plant Science*, *27*, 688–698. https://doi.org/10.1016/j.tplants.2022.01.010

Hanlon, M. T., Vejchasarn, P., Fonta, J. E., Schneider, H. M., McCouch, S. R., & Brown, K. M. (2023). Genome wide association analysis of root hair traits in rice reveals novel genomic regions controlling epidermal cell differentiation. *BMC Plant Biology*, *23*, 6. https://doi.org/10.1186/s12870-022-04026-5

Helliwell, J. R., Miller, A. J., Whalley, W. R., Mooney, S. J., & Sturrock, C. J. (2014). Quantifying the impact of microbes on soil structural development and behaviour in wet soils. *Soil Biology and Biochemistry*, *74*, 138–147. https://doi.org/10.1016/J.SOILBIO.2014.03.009

Helliwell, J. R., Sturrock, C. J., Mairhofer, S., Craigon, J., Ashton, R. W., Miller, A. J., Whalley, W. R., & Mooney, S. J. (2017). The emergent rhizosphere: Imaging the development of the porous architecture at the root-soil interface. *Scientific Reports*, *7*, 14875. https://doi.org/10.1038/s41598-017-14904-w

Helliwell, J. R., Sturrock, C. J., Miller, A. J., Whalley, W. R., & Mooney, S. J. (2019). The role of plant species and soil condition in the structural development of the rhizosphere. *Plant, Cell & Environment*, *42*, 1974–1986. https://doi.org/10.1111/PCE.13529

Horn, R., & Dexter, A. R. (1989). Dynamics of soil aggregation in an irrigated desert loess. *Soil and Tillage Research*, *13*, 253–266. https://doi.org/10.1016/0167-1987(89)90002-0

Islam, M. D. D., Price, A. H., & Hallett, P. D. (2021). Contrasting ability of deep and shallow rooting rice genotypes to grow through plough pans containing simulated biopores and cracks. *Plant and Soil*, *467*, 515–530. https://doi.org/10.1007/S11104-021-05131-4/figures/5

Islam, M. D. D., Price, A. H., & Hallett, P. D. (2023). Effects of root growth of deep and shallow rooting rice cultivars in compacted Paddy soils on subsequent rice growth. *Rice Science*, *30*, 459–472. https://doi.org/10.1016/j.rsci.2023.03.017

Katuwal, S., Norgaard, T., Moldrup, P., Lamandé, M., Wildenschild, D., & de Jonge, L. W. (2015). Linking air and water transport in intact soils to macropore characteristics inferred from X-ray computed tomography. *Geoderma*, *237*, 9–20. https://doi.org/10.1016/j.geoderma.2014.08.006

Koebernick, N., Daly, K. R., Keyes, S. D., George, T. S., Brown, L. K., Raffan, A., Cooper, L. J., Naveed, M.,

Bengough, A. G., Sinclair, I., Hallett, P. D., & Roose, T. (2017). High-resolution synchrotron imaging shows that root hairs influence rhizosphere soil structure formation. *The New Phytologist*, 216, 124–135. https://doi.org/10.1111/NPH.14705

Kutay, M. E., Aydilek, A. H., Masad, E., & Harman, T. (2007). Computational and experimental evaluation of hydraulic conductivity anisotropy in hot-mix asphalt. *International Journal of Pavement Engineering*, 8, 29–43. https://doi.org/10.1080/10298430600819147

Lampayan, R. M., Rejesus, R. M., Singleton, G. R., & Bouman, B. A. M. (2015). Ethylene inhibits rice root elongation in compacted soil via ABA- and auxin-mediated mechanisms. *Field Crops Research*, 170, 95–108. https://doi.org/10.1016/j.fcr.2014.10.013

Liang, S., Wang, Y. H., Zhang, H., Yun, X. Y., & Wu, Y. (2020). Response of root-exuded organic acids in irrigated rice to different water management practices. *Eurasian Soil Science*, 53, 1572–1578. https://doi.org/10.1134/S1064229320110101

Liao, B., Wu, X., Yu, Y., Luo, S., Hu, R., & Lu, G. (2020). Effects of mild alternate wetting and drying irrigation and mid-season drainage on CH_4 and N_2O emissions in rice cultivation. *Science of The Total Environment*, 698, 134212. https://doi.org/10.1016/j.scitotenv.2019.134212

Lu, J., Ookawa, T., & Hirasawa, T. (2000). The effects of irrigation regimes on the water use, dry matter production and physiological responses of paddy rice. *Plant and Soil*, 223, 209–218. https://doi.org/10.1023/A:1004898504550

Lucas, M., Schlüter, S., Vogel, H. J., Vogel, H. J., & Vetterlein, D. (2019). Roots compact the surrounding soil depending on the structures they encounter. *Scientific Reports*, 9, 16236. https://doi.org/10.1038/s41598-019-52665-w

Marin, M., Hallett, P. D., Feeney, D. S., Brown, L. K., Naveed, M., Koebernick, N., Ruiz, S., Bengough, A. G., Roose, T., & George, T. S. (2022). Impact of root hairs on microscale soil physical properties in the field. *Plant and Soil*, 476, 491–509. https://doi.org/10.1007/S11104-022-05530-1/figures/8

Maruyama, T. K. (1997). *Physical and chemical processes of soil related to paddy drainage*. Shinzansha Sci. ans Tech. Shinzansha Sci. & Tech.

Materechera, S. A., Dexter, A. R., & Alston, A. M. (1992). Formation of aggregates by plant roots in homogenised soils. *Plant and Soil*, 142, 69–79.

Mitchell, J. K., & Soga, K. (2005). *Fundamentals of soil behavior*. John Wiley and Sons, Inc.

Mooney, S. J., Pridmore, T. P., Helliwell, J., & Bennett, M. J. (2012). Evaluation of growth, yield, and water productivity of paddy rice with water-saving irrigation and optimization of nitrogen fertilization. *Plant and Soil*, 352, 1–22. https://doi.org/10.1007/s11104-011-1039-9

Moreno-Espíndola, I. P., Rivera-Becerril, F., de Jesús Ferrara-Guerrero, M., & De León-González, F. (2007). Role of root-hairs and hyphae in adhesion of sand particles. *Soil Biology and Biochemistry*, 39, 2520–2526. https://doi.org/10.1016/J.SOILBIO.2007.04.021

Naveed, M., Brown, L. K., Raffan, A. C., George, T. S., Bengough, A. G., Roose, T., Sinclair, I., Koebernick, N., Cooper, L., & Hallett, P. D. (2018). Rhizosphere-scale quantification of hydraulic and mechanical properties of soil impacted by root and seed exudates. *Vadose Zone Journal*, 17, 1–12. https://doi.org/10.2136/VZJ2017.04.0083

Niu, W. Q., Jia, Z. X., Zhang, X., & Shao, H. B. (2012). Effects of soil rhizosphere aeration on the root growth and water absorption of tomato. *CLEAN – Soil Air, Water*, 40, 1364–1371. https://doi.org/10.1002/CLEN.201100417

Nong, R., Wan, Y., Ding, Y., Chai, M., & Zhu, L. (2023). Effects of root systems on crack formation: Experiments, modeling, and analyses. *Soil and Tillage Research*, 233, 105784. https://doi.org/10.1016/j.still.2023.105784

Norhidayah, A. H., Mahmud, M. Z. H., & Ramadhansyah, P. J. (2014). Evaluation of growth, yield, and water productivity of Paddy Rice with water-saving irrigation and optimization of nitrogen fertilization. *Advances in Materials Research*, 911, 443–448.

Norton, G. J., Shafaei, M., Travis, A. J., Deacon, C. M., Danku, J., Pond, D., Cochrane, N., Lockhart, K., Salt, D., Zhang, H., Dodd, I. C., Hossain, M., Islam, M. R., & Price, A. H. (2017). Impact of alternate wetting and drying on rice physiology, grain production, and grain quality. *Field Crops Research*, 205, 1–13. https://doi.org/10.1016/j.fcr.2017.01.016

Passioura, J. B. (1991). Soil structure and plant growth. *Australian Journal of Soil Research*, 29, 717–728.

Phalempin, M., Lippold, E., Vetterlein, D., & Schlüter, S. (2021). Soil texture and structure heterogeneity predominantly governs bulk density gradients around roots. *Vadose Zone Journal*, 20, e20147. https://doi.org/10.1002/vzj2.20147

Pires, L. F., Bacchi, O. O. S., & Reichardt, K. (2007). Assessment of soil structure repair due to wetting and drying cycles through 2D tomographic image analysis. *Soil and Tillage Research*, 94, 537–545. https://doi.org/10.1016/j.still.2006.10.008

Pires, L. F., Cooper, M., Cássaro, F. A. M., Reichardt, K., Bacchi, O. O. S., & Dias, N. M. P. (2008). Micromorphological analysis to characterize structure modifications of soil samples submitted to wetting and drying cycles. *Catena*, 72, 297–304. https://doi.org/10.1016/j.catena.2007.06.003

Pires, L. F., Roque, W. L., Rosa, J. A., & Mooney, S. J. (2019). 3D analysis of the soil porous architecture under long term contrasting management systems by X-ray computed tomography. *Soil and Tillage Research*, 191, 197–206. https://doi.org/10.1016/j.still.2019.02.018

Schindelin, J., Arganda-Carreras, I., Frise, E., Kaynig, V., Longair, M., Pietzsch, T., Preibisch, S., Rueden, C., Saalfeld, S., Schmid, B., Tinevez, J. Y., White, D. J., Hartenstein, V., Eliceiri, K., Tomancak, P., & Cardona, A. (2012). Fiji: An open-source platform for biological-image analysis. *Nature Methods*, 9, 676–682. https://doi.org/10.1038/nmeth.2019

Shrestha, R., Al-Shugeairy, Z., Al-Ogaidi, F., et al. (2014). Comparing simple root phenotyping methods on a core set of rice genotypes. *Plant Biology*, 16, 632–642. https://doi.org/10.1111/plb.12096

Vogel, H. J. (1997). Morphological determination of pore connectivity as a function of pore size using serial sections. *European Journal of Soil Science*, 48, 365–377. https://doi.org/10.1111/J.1365-2389.1997.TB00203.X

Willatt, S. T., & Sulistyaningsih, N. (1990). Effect of plant roots on soil strength. *Soil and Tillage Research*, 16, 329–336. https://doi.org/10.1016/0167-1987(90)90068-O

Yang, J., & Zhang, J. (2010). Crop management techniques to enhance harvest index in rice. *Journal of Experimental Botany*, *61*, 3177–3189. https://doi.org/10.1093/jxb/erq112

Yao, F., Huang, J., Cui, K., Nie, L., Xiang, J., Liu, X., Wu, W., Chen, M., & Peng, S. (2012). Agronomic performance of high-yielding rice variety grown under alternate wetting and drying irrigation. *Field Crops Research*, *126*, 16–22. https://doi.org/10.1016/j.fcr.2011.09.018

Yoshida, S., & Hallett, P. D. (2008). Impact of hydraulic suction history on crack growth mechanics in soil. *Water Resources Research*, *44*, W00C01. https://doi.org/10.1029/2007WR006055

Young, I. M. (1995). Variation in moisture contents between bulk soil and the rhizosheath of wheat (*Triticum aestivum* L. cv. Wembley). *The New Phytologist*, *130*, 135–139. https://doi.org/10.1111/J.1469-8137.1995.TB01823.X

Zhao, K., Tung, C. W., Eizenga, G. C., Wright, M. H., Ali, M. L., Price, A. H., Norton, G. J., Islam, M. R., Reynolds, A., Mezey, J., McClung, A. M., Bustamante, C. D., & McCouch, S. R. (2011). Genome-wide association mapping reveals a rich genetic architecture of complex traits in *Oryza sativa*. *Nature Communications*, *2*, 1–10. https://doi.org/10.1038/ncomms1467

SUPPORTING INFORMATION

Additional supporting information can be found online in the Supporting Information section at the end of this article.